Chapter II

CONSTANT Q -- WAVE PROPAGATION AND ATTENUATION

A fundamental feature associated with the propagation of stress waves in all real materials is the absorption of energy and the resulting change in the shape of transient waveforms. Although a large number of papers have been written on the absorption of seismic waves in rocks, little, if any, general agreement exists about even the most fundamental properties of the processes involved. Table 2.1 shows a summary of the basic features of some of the different attenuation theories.

Early laboratory work on absorption in rocks showed the loss per cycle or wavelength to be essentially independent of frequency. Since at that time no known linear theory could fit this observation, Born [1941] proposed that the loss was due to rate-independent friction of the same kind as observed when two surfaces slide against each other. Kolsky [1956] and Lomnitz [1957] gave linear descriptions of the absorption that could account for the observed frequency-independence and were also consistent with other independent observations of the transient creep in rocks and the change in shape of pulses propagating through thin rods. Despite this and the fact that a satisfactory nonlinear friction model for attenuation has never been developed to the point where meaningful predictions could be made about the propagation of waves, nonlinear friction is commonly assumed to be the dominant attenuation mechanism, especially in crustal rocks [McDonal et al., 1958, Knopoff, 1964; White, 1966; Gordon and Davis, 1968; Lockner et al., 1977; Johnston and Toksoz, 1977].

A different type of theory for attenuation has been advocated by Ricker [1953, 1977]. In his model the absorption is described by adding a single term to the wave equation. Because of this simplicity, the theory of the propagation of transient waves has been further developed than for the other theories. For this reason, wavelets based on the Ricker theory have been commonly used in the computation of synthetic seismograms [Boore et al., 1971; Munasinghe and Farnell, 1973], although the frequency-dependence of Q that is implied by the model contradicts practically all experimental observations.

Property	Theory: Friction	Theory: Voigt-Ricker	Theory: NCQ Band-Limited Near-Constant Q	Theory: CQ Linear Constant Q
Linearity	Nonlinear, velocity and Q depend on amplitude	Linear	Linear	Linear
Frequency dependence of Q	Independent	$1/Q \propto \omega$	Nearly independent in a frequency band	Independent
Frequency dependence of phase velocity	Independent	Independent at low frequencies	$C/C_0 \approx 1 + (1/\pi Q) \ln (\omega/\omega_0)$	$C/C_0 = (\omega/\omega_0)^\gamma$ $1/Q = \tan(\pi\gamma)$
Transient creep	None	$\Psi(t) \propto e^{-at}$	$\Psi(t) \approx (1/M_0)[1 + (2/\pi Q) \ln (1 + at)]$	$\Psi(t) \propto t^{2\gamma}$
Pulse broadening	Distorted or acausal	$\tau \propto T^{1/2}$	$\tau \mathrel{\tilde{\propto}} T$	$\tau \propto T$
References	*Born* [1941] *Knopoff* [1964] *White* [1966] *Walsh* [1966] *Lockner et al.* [1977] *Johnston and Toksöz* [1977] *Gordon and Davis* [1968]	*Voigt* [1892] *Ricker* [1953, 1977] *Collins* [1960] *Clark and Rupert* [1960] *Jaramillo and Colvin* [1970] *Balch and Smolka* [1970]	*Kolsky* [1956] *Lomnitz* [1957] *Futterman* [1962] *Azimi et al.* [1968] *Strick* [1967, 1970] *Liu et al.* [1976] *Kanamori and Anderson* [1977] *Minster* [1978*a*]	*Bland* [1960] *Strick* [1967] This paper

TABLE 2.1. Comparison of attenuation theories.

In this paper, we will discuss some of the data Ricker interpreted as in support of his theory.

Recently, there has been renewed interest in the effects of anelasticity on wave propagation in rocks. Liu et al. [1976] found that the change in the elastic moduli implied by attenuation over the frequency range covered by seismic body waves and free oscillations, was about an order of magnitude greater than the uncertainty in the measurements. The models used by Liu et al. [1976], as well as all of the other nearly constant Q (NCQ) models, have included at least one parameter that is in some way related to the range of frequencies over which the model gives Q nearly independent of frequency. How this cutoff is chosen appears to be quite arbitrary and the physical implications of the cutoff parameters are different between the models of Lomnitz [1957], Futterman [1962], Strick [1967], and Liu et al. [1976].

In this paper a linear description of the attenuation is given, that features Q exactly independent of frequency, without any cutoffs. The constant Q (CQ) model is mathematically much simpler than any of the NCQ models; it is completely specified by two parameters, i. e. phase velocity at an arbitrary reference frequency, and Q.

Most of the NCQ papers have described wave phenomena in the frequency-domain and have restricted their analysis to cases where Q is large ($Q > 30$). In contrast, the simplicity of the CQ description allows the derivation of exact analytical expressions for the various frequency-domain properties, such as the complex modulus, phase velocity, and the attenuation coefficient, that are valid over any range of frequencies and for any positive value of Q. In this paper more emphasis will be placed on the time-domain description of transient phenomena, and exact expressions for the creep and relaxation functions and scaling relations for the transient wave pulse will be given. In addition, approximate expressions will be given for the impulse response, as a function of time, that results from a delta-function excitation.

We will also show that when the frequency range is restricted and the losses are small, the results obtained from the various NCQ theories approach the same limit as those obtained from the CQ theory.

Definitions and Background

Seismic attenuation is commonly characterized by the quality parameter Q. It is most often defined in terms of the maximum energy stored during a cycle, divided by the energy lost during the cycle. When the loss is large this definition becomes impractical; O'Connell and Budiansky [1978] suggested a definition in terms of the mean stored energy W and the energy loss ΔW, during a single cycle of sinusoidal deformation.

$$Q = \frac{4\pi W}{\Delta W} \tag{2.1}$$

When this definition is used, Q is related to the phase angle between stress and strain, δ, according to

$$\frac{1}{Q} = \tan \delta \tag{2.2}$$

The fact that amplitude-dependence of the propagation velocity and Q at strains less than 10^{-6} has not been observed, strongly suggests that at these amplitudes the material response is dominated by linear effects, or in other words, the strain that results from a superposition of two stress functions is equal to the sum of the strains that result from the application of each stress function separately. When two effects are linearly related, the relationship may be expressed through a convolution. Thus the relationship between stress and strain in a linear material may be expressed as

$$\sigma(t) = m(t) * \varepsilon(t) \tag{2.3}$$

$$\varepsilon(t) = s(t) * \sigma(t) \tag{2.4}$$

where $\sigma(t)$ is the stress as a function of time, $\varepsilon(t)$ is the strain, and m(t) and s(t) are real functions that vanish for negative time. The convolution operator $*$ is defined by

$$f(t) * g(t) = \int_{-\infty}^{\infty} f(t-t')g(t')dt' \tag{2.5}$$

The relationship between stress and strain given in (2.3) and (2.4) was first given by Boltzmann [1876]. Our notation differs from Boltzmann's original notation only in that the functions m(t) and s(t) may include generalized functions such as the Dirac delta function or its derivatives. Combination of (2.3) and (2.4) implies that m(t) and s(t) must satisfy the condition

$$\delta(t) = m(t) * s(t) \tag{2.6}$$

where $\delta(t)$ is the Dirac delta function.

Manipulations involving convolutions are usually facilitated by the use of the Fourier transform. We will use lower case letters to designate functions of time and capital letters for their Fourier transforms according to the definition

$$F(\omega) = \int_{-\infty}^{\infty} f(t)\, e^{-i\omega t} dt \tag{2.7}$$

The inverse Fourier transform is then given by

$$f(t) = \frac{1}{2\pi} \int_{-\infty}^{\infty} F(\omega)\, e^{i\omega t} d\omega \tag{2.8}$$

Bracewell [1965] gives a discussion of the formalism required for the extension to generalized functions.

Using the convolution theorem [Bracewell, 1965; p. 108], equations (2.3), (2.4) and (2.6) may be rewritten:

$$\Sigma(\omega) = M(\omega)E(\omega) \tag{2.9}$$

$$E(\omega) = S(\omega)\Sigma(\omega) \tag{2.10}$$

$$1 = M(\omega)S(\omega) \tag{2.11}$$

where $\Sigma(\omega)$ is the Fourier transform of the stress, $E(\omega)$ is the Fourier transform of the strain, and $M(\omega)$ and $S(\omega)$ are the Fourier transforms of $m(t)$ and $s(t)$. Thus, the stress and the strain are in the frequency-domain related through a multiplication by a modulus $M(\omega)$ or compliance $S(\omega)$ just as in the purely elastic case, the only difference being that the modulus may be complex and frequency-dependent. This relationship is commonly referred to as the correspondence principle. By the substitution of a unit step function into (2.3) and (2.4), it is easily shown that $m(t)$ and $s(t)$ are the first time derivatives of the relaxation and creep functions, where the relaxation function, $\bar{\Psi}(t)$, is the stress that results from a unit step in strain, and the creep function, $\Psi(t)$, is the strain that results from a unit step in stress.

When the stress-strain relations are combined with the equilibrium equation, the resulting one-dimensional wave equation has a solution that may be written in a form analogous to the classical case:

$$U(t,x) = \exp[i(\omega t - kx)] \tag{2.12}$$

where

$$k = \omega \left(\frac{\rho}{M(\omega)}\right)^{\frac{1}{2}} \tag{2.13}$$

and ρ is the density of the material.

The Constant Q Model

The development so far has been completely general; no assumptions other than linearity and causality have been made about the properties of the material. We will now examine a particular form for the stress-strain relationships and show that it leads to a Q that is independent of frequency. Frequency-independent Q implies that the loss per cycle is independent of the time scale of oscillation; therefore it might seem reasonable to try a material that has a creep function that plots as a straight line on a log-log plot, or

$$\Psi(t) \propto t^b$$

For the sake of convenience in subsequent manipulations, we will use a creep function of the form

$$\Psi(t) = \frac{1}{M_0\Gamma(1+2\gamma)}\left(\frac{t}{t_0}\right)^{2\gamma} \qquad t > 0 \tag{2.14}$$

$$\Psi(t) = 0 \qquad t < 0$$

Γ is the gamma function which in all cases of interest to us has a value close to unity and t_0 is an arbitrary reference time introduced so that when t has the dimension of time, M_0 will have the dimension of modulus. Some of the properties of a material that has this creep function are discussed by Bland [1960, p.54]. Response functions of this form have also been used to model dielectric losses in solids [Jonscher, 1977]. Differentiation of the expression in (2.14) yields

$$s(t) = \frac{2\gamma}{M_0\Gamma(1+2\gamma)}\left(\frac{t}{t_0}\right)^{2\gamma}\frac{1}{t} \qquad t > 0 \tag{2.15}$$

$$s(t) = 0 \qquad t < 0$$

Taking the Fourier transform we get

$$S(\omega) = \frac{1}{M_0}\left(\frac{i\omega}{\omega_0}\right)^{-2\gamma} \tag{2.16}$$

where

$$\omega_0 = \frac{1}{t_0} \tag{2.17}$$

Using (2.11) we get

$$M(\omega) = M_0\left(\frac{i\omega}{\omega_0}\right)^{2\gamma} = M_0\left|\frac{\omega}{\omega_0}\right|^{2\gamma}\exp[i\pi\gamma\ \mathrm{sgn}(\omega)] \tag{2.18}$$

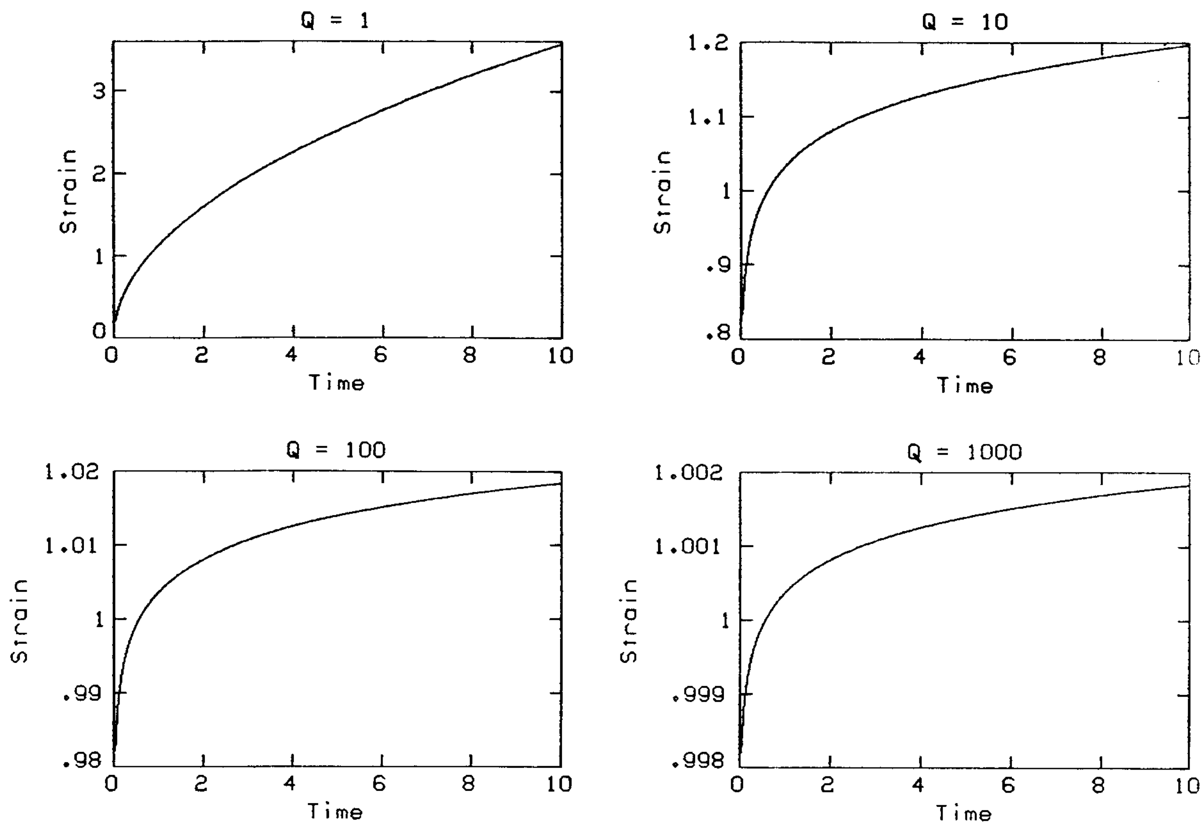

FIG. 2.1. The constant Q creep function as given by equation (2.14), in units of $1/M_0$, plotted versus time in units of t_0.

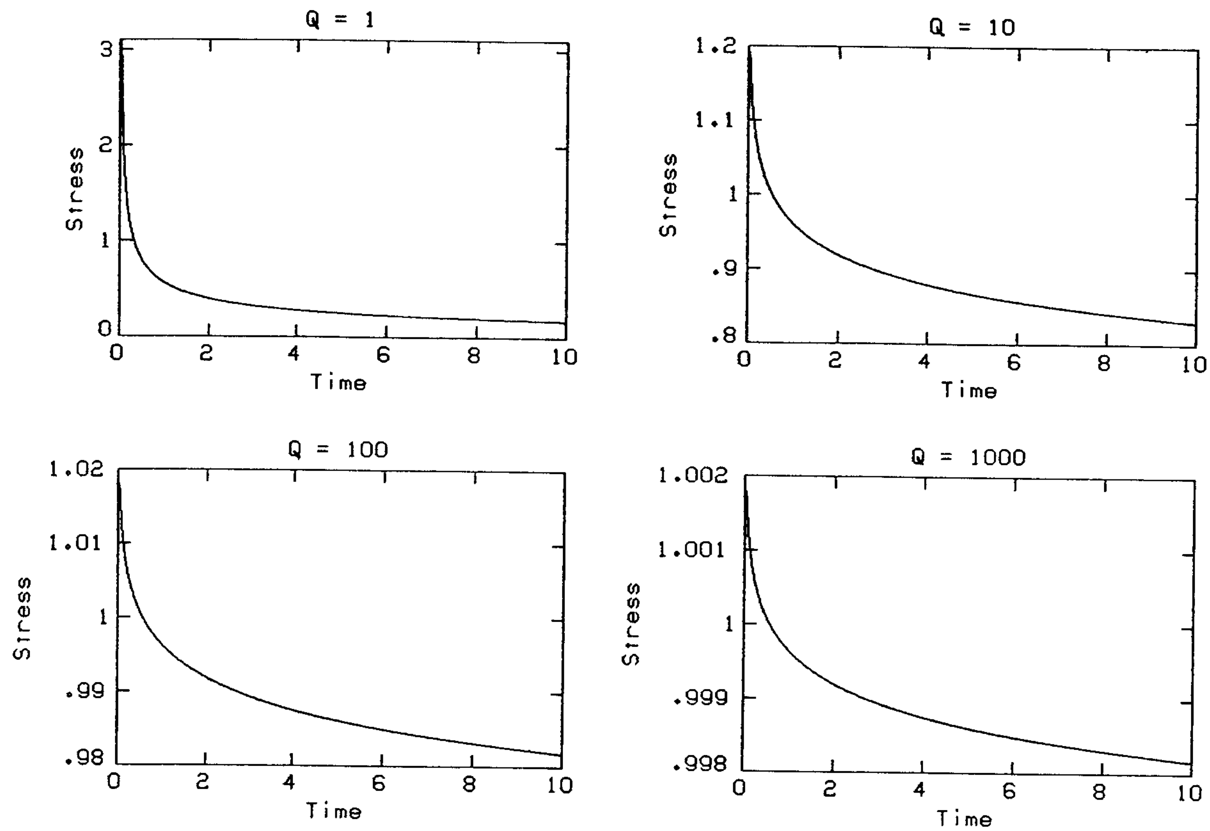

FIG. 2.2. The constant Q relaxation function as given by equation (2.20), in units of M_0, plotted versus time in units of t_0.

where

$$\mathrm{sgn}(\omega) = 1 \qquad \omega > 0 \tag{2.19}$$

$$\mathrm{sgn}(\omega) = -1 \qquad \omega < 0$$

Taking the inverse Fourier transform of $M(\omega)$ and integrating, we get the relaxation function

$$\bar{\Psi}(t) = \frac{M_0}{\Gamma(1-2\gamma)}\left(\frac{t}{t_0}\right)^{-2\gamma} \qquad t > 0 \tag{2.20}$$

$$\bar{\Psi}(t) = 0 \qquad t < 0$$

Figure 2.1 shows a plot of the constant Q creep function (2.14), and figure 2.2, of the relaxation function (2.20), for several values of Q. Equation (2.18) shows that the argument of the modulus and thus the phase angle beween the stress and the strain, is independent of frequency; therefore, it follows from the definition of Q (2.2) that Q is independent of frequency:

$$\frac{1}{Q} = \tan(\pi\gamma) \tag{2.21}$$

or

$$\gamma = \frac{1}{\pi}\tan^{-1}\left(\frac{1}{Q}\right) \simeq \frac{1}{\pi Q} \tag{2.22}$$

The approximation is valid when $Q^{-2} \ll 1$. Since both the creep and relaxation functions vanish for negative time, no strain can precede applied stress, nor can any stress precede applied strain; the material is causal.

To investigate the propagation of waves in the constant Q material, the modulus given by (2.18) may be substituted into the solution to the one-dimensional wave equation, given by (2.12) and (2.13); the result may be written as

$$U(t,x) = e^{-\alpha x} e^{i\omega(t-x/c)} \qquad (2.23)$$

where

$$c = c_0 \left| \frac{\omega}{\omega_0} \right|^{\gamma} \qquad (2.24)$$

$$\alpha = \tan\left(\frac{\pi\gamma}{2}\right) \operatorname{sgn}(\omega) \frac{\omega}{c} \qquad (2.25)$$

$$c_0 = \frac{\left(\frac{M_0}{\rho}\right)^{1/2}}{\cos\left(\frac{\pi\gamma}{2}\right)} \qquad (2.26)$$

Since c is slightly dependent on frequency, constant Q is not exactly equivalent to assuming that α is proportional to frequency, as is often assumed in the literature. It is clear from (2.24) that c_0 is simply the phase velocity at the arbitrary reference frequency ω_0. In the final section of the paper, we discuss the low- and high-frequency limits for the phase velocity and the modulus, and the short- and long-term behavior of the creep function.

An alternative to (2.23) is to write the solution to the wave equation as

$$U(x,t) = \exp\left[i\omega \left(t - \frac{x}{c_s (i\omega)^{\gamma}} \right) \right] \qquad (2.27)$$

where c_s is a constant related to M_0 by

$$c_s = \left(\frac{M_0}{\rho}\right)^{1/2} \omega_0^{-\gamma} \qquad (2.28)$$

Use of the complex velocity notation, as in (2.27), often simplifies the algebra, e.g. in the derivation of reflection coefficients or when modeling wave propagation in two or three dimensions.

As most wave phenomena encountered in seismology are transient in nature, a time-domain description of wave propagation is often more useful for modeling or comparison with data than a frequency-domain description. The waveform that results from a delta-function source, the impulse response, is particularly useful since the waveform that results from an arbitrary source is obtained by simply convolving the source with the impulse response. The Fourier transform of the impulse response, b(t), is obtained by omitting the $i\omega t$ term in (2.12) or (2.23):

$$B(\omega) = e^{-\alpha x} e^{-i\omega x/c} \tag{2.29}$$

By the substitution of (2.24) and (2.25) into (2.29), we get

$$B(\omega) = \exp\left\{- \frac{x\omega_0}{c_0} \left|\frac{\omega}{\omega_0}\right|^{1-\gamma} \left[\tan\left(\frac{\pi\gamma}{2}\right) + i \,\mathrm{sgn}(\omega)\right]\right\} \tag{2.30}$$

The impulse response may be obtained by taking the inverse Fourier transform of $B(\omega)$ given by (2.30). Although we do not have an analytical expression for b(t), we will present a useful approximate relation and some exact scaling relations. We will rewrite (2.30) as

$$B(\omega) = B_1(\omega_1) \tag{2.31}$$

where

$$\omega_1 = t_1\omega \tag{2.32}$$

$$t_1 = t_0\left(\frac{x\omega_0}{c_0}\right)^{\beta} \tag{2.33}$$

$$\beta = \frac{1}{1-\gamma} \simeq 1 + \frac{1}{\pi Q} \tag{2.34}$$

and

$$B_1(\omega) = \exp\left\{-|\omega|^{1-\gamma}\left[\tan\left(\frac{\pi\gamma}{2}\right) + i \,\mathrm{sgn}(\omega)\right]\right\} \tag{2.35}$$

It now follows from the similarity theorem [Bracewell, 1965; p. 101] that for any homogeneous material, the impulse response at any distance x from the source will be given by

$$b(t,x) = \frac{1}{t_1} b_1\left(\frac{t}{t_1}\right) \qquad (2.36)$$

Equations (2.36) and (2.33) imply that in a given material, the traveltime T, the pulse width τ, and the pulse amplitude A are related according to

$$T \propto \tau \propto \frac{1}{A} \propto \left(\frac{x}{c_0}\right)^{\beta} \qquad (2.37)$$

where any consistent operational definitions for the traveltime and pulse width may be used. The proportionality between traveltime and pulse width may be expressed as

$$\tau = C(Q)\frac{T}{Q} \qquad (2.38)$$

where C(Q) is a function that depends only on Q. We will show that C(Q) is nearly constant for Q > 20. Figure 2.3 shows a plot of the function $b_1(t)$, for several values of Q.

In order to illustrate the scaling relations, seismograms due to impulsive sources at several distances are plotted on a common set of axes in figure 2.4. Figure 2.5 shows the same information but scaled according to distance, by dividing the time by the distance and multiplying the displacement by the distance. Velocity dispersion has the effect of delaying the pulses from the more distant sources more than would be expected for a constant propagation velocity. To further illustrate the dispersion, figure 2.6 shows the results of the same kind of numerical experiment as figure 2.5, for a Q of 1000 and covering a larger range of distances. It may be concluded from figures 2.5 and 2.6 that the dispersion due to the anelasticity is directly observable in the time domain when the traveltime, in a homogeneous material, can be measured to within half a pulse width over a ratio of 10 in distance. This applies to high Q as well as to low Q materials. To measure this effect

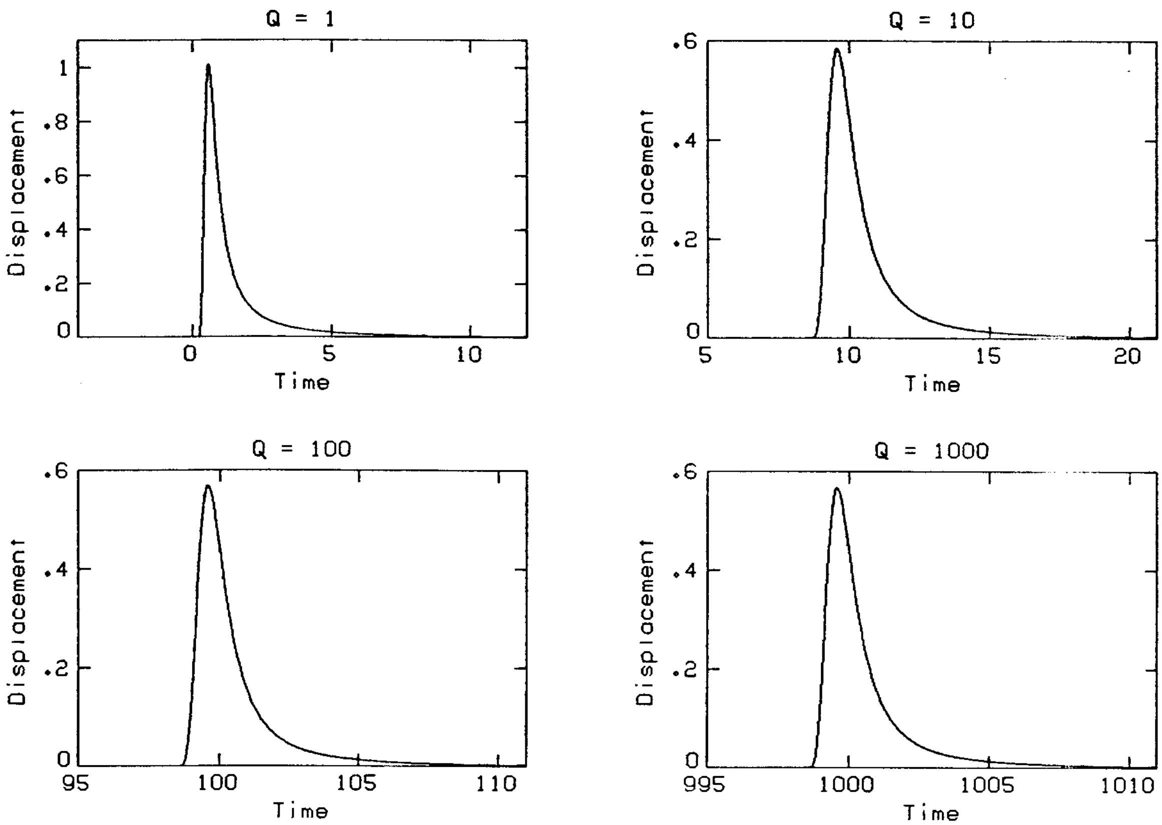

FIG. 2.3. The waveform b(t), resulting from a unit impulse plane-wave source at $x = Qc_0$, is plotted versus time in units of t_0. The waveform is computed using a numerical FFT algorithm.

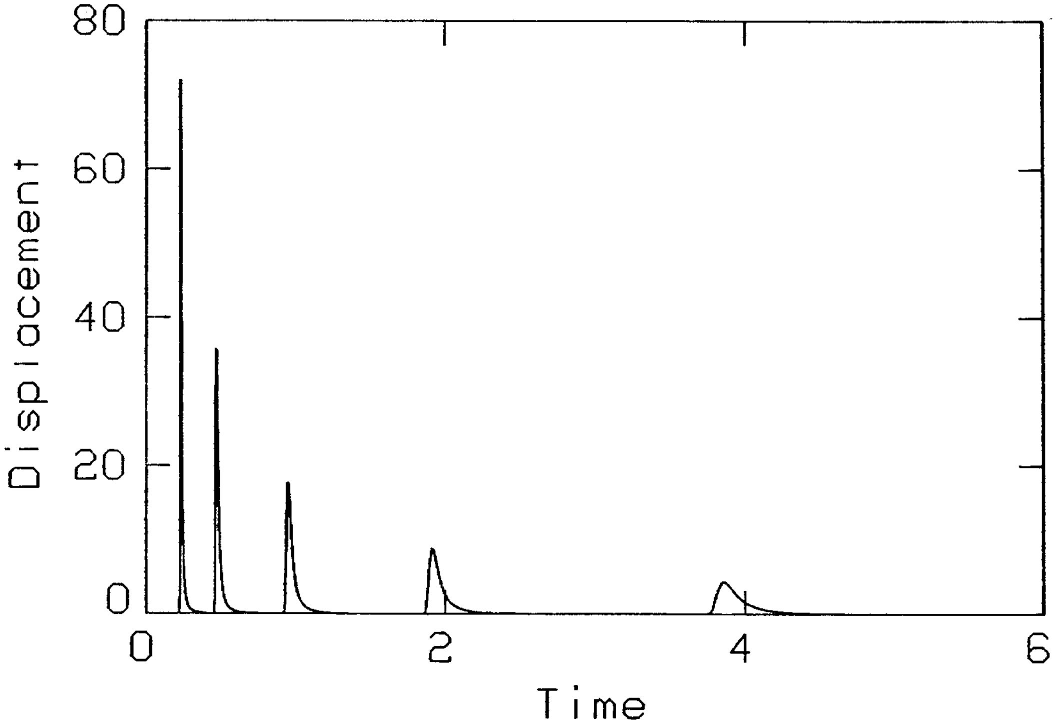

FIG. 2.4. Seismograms resulting from sources at distances of 0.25, 0.5, 1, 2 and 4 times c_0. Q is 30.

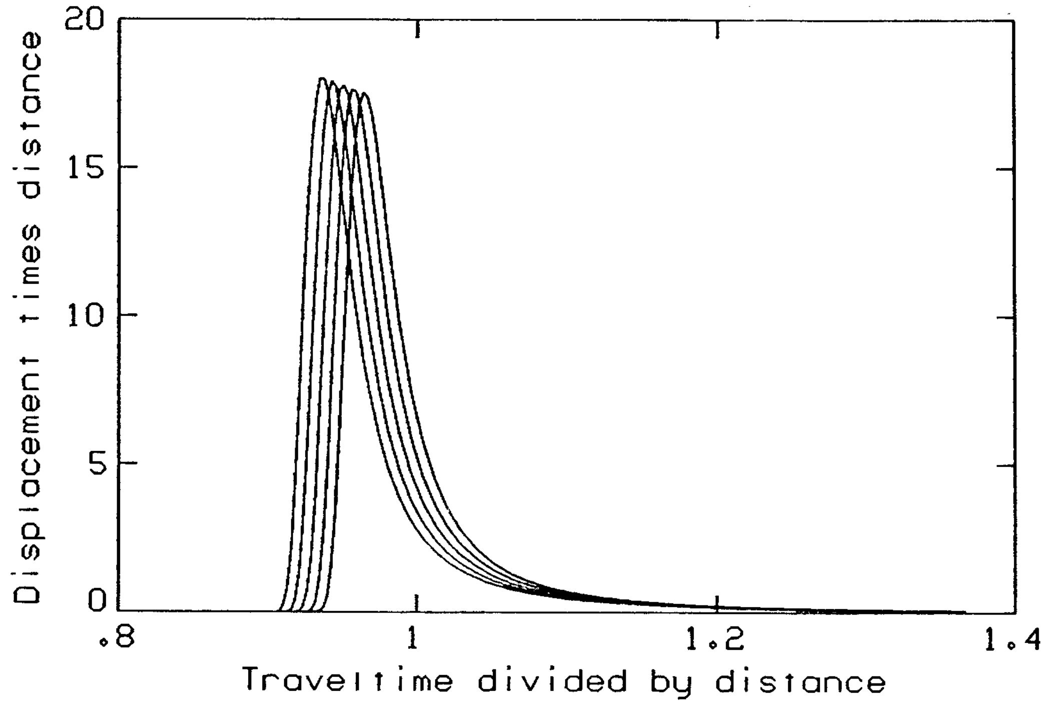

FIG. 2.5. Same seismograms as in figure 2.4, but plotted as displacement times distance versus time divided by distance. The seismograms do not overlap due to velocity dispersion.

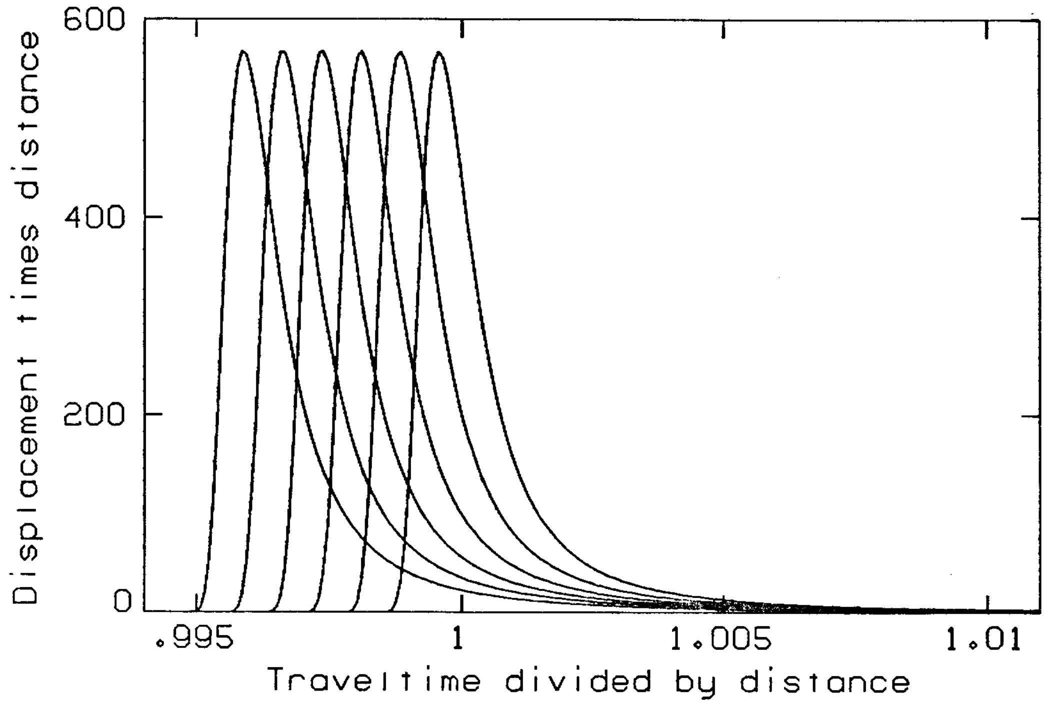

FIG. 2.6. Seismograms resulting from sources at distances of 0.01, 0.1, 1, 10, 100, and 1000 times c_0 plotted in the same manner as in figure 2.5, for Q = 1000. This shows that the dispersion effect, relative to the pulse width, is independent of Q when Q >> 1.

in the earth would, however, require a careful control over the spatial variation in velocity.

The required control may be obtained when the wave travels the same path more than once. Waves reflected off the core-mantle interface may satisfy this condition for stations near the source. Assuming an average Q = 160 and a traveltime of 936 seconds for one pass of ScS [Jordan and Sipkin, 1977], we obtain by a substitution into (2.34) a value for β = 1.0020. Equation (2.37) implies then that doubling the distance will result in a total traveltime of 1874.6 seconds for ScS_2, which is 2.6 seconds longer than would be expected if the dispersion were not present.

Approximations for Time-Domain Wavelets

So far we have made no assumptions about the value of Q (other than Q > 0), or the ranges of frequencies and traveltimes involved. Although we have been able to derive exact expressions for all frequency-domain properties of the wave propagation, we do not have exact analytical expressions for time-domain wavelets or impulse responses. While modern computer techniques (e.g. the fast-Fourier-transform algorithm) make it relatively easy to transform data to the frequency domain and back, it is still useful to study the time-domain waveform, especially since much of earthquake data is still recorded in an analog form. The need for a convenient time-domain representation is demonstrated by the fact that wavelets based on the Voigt-Ricker model are often used by workers who do not accept the frequency-dependence of Q implied by that model [e.g. Boore et al., 1971; Munasinghe and Farnell, 1973].

Strick [1967] applied the causality requirement to the propagation of a wave pulse, and found a form for the propagation function that satisfies this requirement. The constant Q transfer function (2.23), is a special case of Strick's function. Later Strick [1970] used the method of steepest descent to approximate the time-domain impulse response. His expression has, in the notation used in this paper, the form

$$b_s(t,x) = \left\{2\pi\gamma t\left[\frac{(1-\gamma)x}{c_s t}\right]^{-1/\gamma}\right\}^{-\frac{1}{2}} \exp\left\{-\frac{\gamma}{(1-\gamma)}t\left[\frac{(1-\gamma)x}{c_s t}\right]^{1/\gamma}\right\}$$

where $b_s(t,x)$ denotes Strick's approximation to the impulse response, and c_s is defined by (2.28). By rearranging this expression, it may be written as

$$b_s(t,x) = \left(\frac{x}{c_s}\right)^{-\beta} t_s^{-(\gamma+1)/2\gamma}[2\pi\gamma(1-\gamma)^{-1/\gamma}]^{-\frac{1}{2}}$$

$$\exp[-\gamma(1-\gamma)^{(1-\gamma)/\gamma}t_s^{1-1/\gamma}] \qquad (2.39)$$

where

$$t_s = t\left(\frac{x}{c_s}\right)^{-\beta}$$

By differentiation we get the approximation for the differentiated impulse response, $b_{sv}(t,x)$:

$$b_{sv}(t,x) = \left(\frac{x}{c_s}\right)^{-\beta} b_s(t,x)\left[(1-\gamma)^{1/\gamma}t_s^{-1/\gamma} - \frac{\gamma+1}{2\gamma t_s}\right] \qquad (2.40)$$

It is evident from inspection of these expressions that they do obey the correct scaling relations given by (2.37). Figures 2.7 and 2.8 show a comparison between the waveshapes computed by the fast-Fourier-transform-method and those computed using the steepest-descent approximation. They show an excellent agreement for the early part of the pulse, which includes most of the higher-frequency information, while the steepest-descent approximation underestimates the low-frequency amplitudes in the later part of the pulse. This is not surprising since the assumptions involved in the steepest descent approximation break down at very low frequencies. This agreement contrasts with the result of Minster [1978a], who in his Figure 3 shows significant differences between arrivals computed using FFT methods and those computed using analytical expansions.

So far we have only considered the pulse propagation in homogeneous materials and given scaling relations applicable to materials with the same value of Q. As the waveshapes plotted in figure 2.3 show a great deal of similarity for different values of Q, it should be possible to give scaling

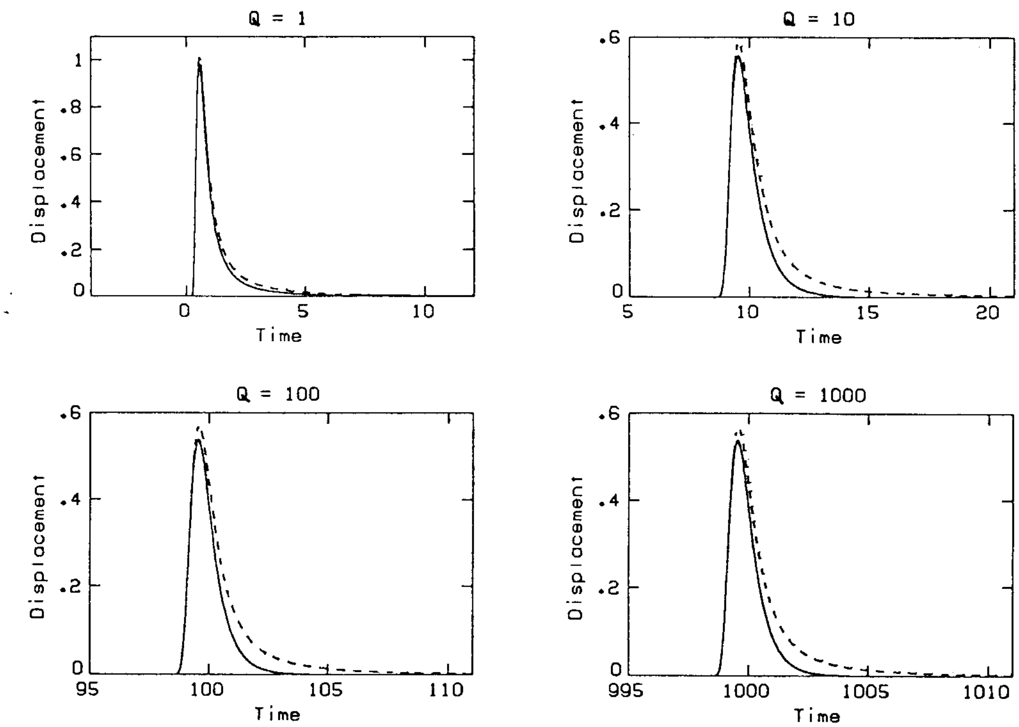

FIG. 2.7. Comparison of waveforms computed using equation (2.39) (solid line), to the waveforms from figure 2.3 (dashed).

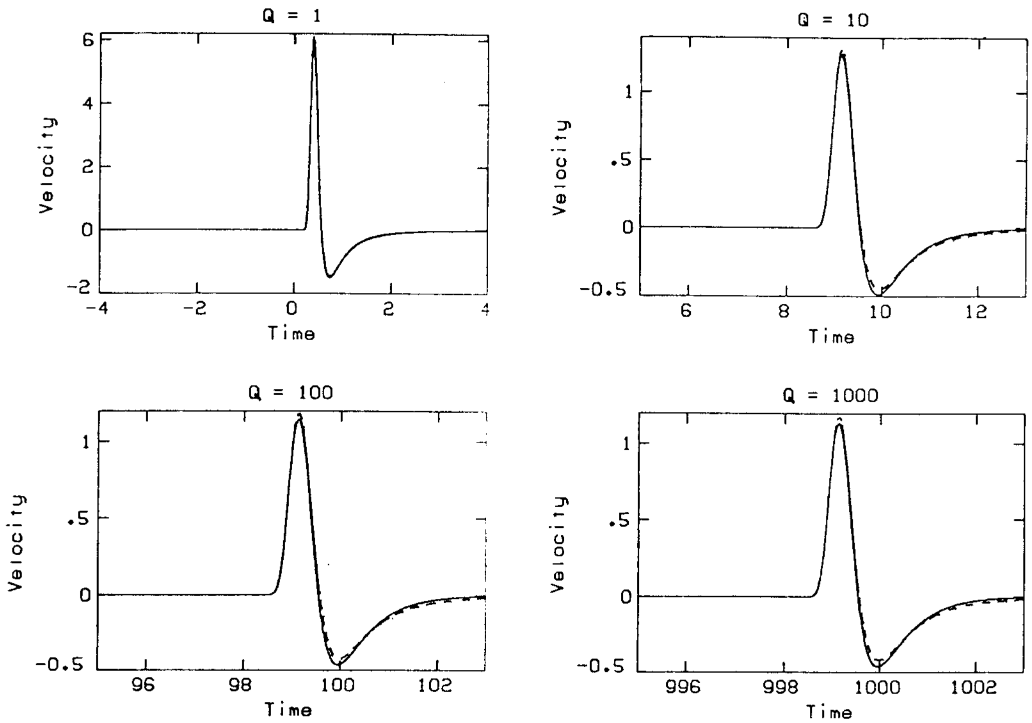

FIG. 2.8. Comparison of waveforms computed using equation (2.40) (solid line), to waveforms computed using numerical FFT algorithms (dashed).

relations for different values of Q as well as for different distances.

When $Q^{-2} << 1$, the tangents in (2.22) and (2.25) may be replaced by their arguments. Thus (2.23) and (2.25) may be written as

$$B(\omega) \simeq \exp\left\{ - \frac{x|\omega|}{2Qc} - i\omega \frac{x}{c} \right\} \tag{2.41}$$

where

$$c \simeq c_0 \left| \frac{\omega}{\omega_0} \right|^{1/\pi Q} \tag{2.42}$$

By use of the Maclaurin-series expansion of the exponential function, equation (2.42) may be written as

$$\frac{c}{c_0} = 1 + \frac{1}{\pi Q} \ln\left|\frac{\omega}{\omega_0}\right| + \frac{1}{2!}\left[\frac{1}{\pi Q} \ln\left|\frac{\omega}{\omega_0}\right|\right] + \ldots\ldots \tag{2.43}$$

When all the frequencies of interest satisfy the condition

$$\frac{1}{\pi Q} \ln\left|\frac{\omega}{\omega_0}\right| << 1 \tag{2.44}$$

sufficient precision may be maintained by only including the first two terms of the expansion given in (2.43). The result is the dispersion relation given by many of the NCQ papers [e.g. Kanamori and Anderson, 1977]. Using the approximation indicated in (2.43), and dropping all terms involving the second or higher powers of 1/Q, equation (2.41) becomes

$$B'(\omega) = \exp\left\{- \frac{x\omega}{c_0}\left[\frac{\text{sgn}(\omega)}{2Q} + i - \frac{i}{\pi Q} \ln\left|\frac{\omega}{\omega_0}\right|\right]\right\} \tag{2.45}$$

The similarity and shift theorems [Bracewell, 1965; p. 101] may now be used to relate the approximate impulse response b'(t) that has $B'(\omega)$ as its Fourier transform, as indicated by the following relations:

$$b'(t) = rb_1'(t') \qquad (2.46)$$

where

$$t' = rt - Q + \frac{1}{\pi} \ln\frac{r}{\omega_0} \qquad (2.47)$$

$$r = \frac{c_0 Q}{x} \qquad (2.48)$$

and $b_1'(t)$ is the inverse Fourier transform of

$$B_1'(\omega') = \exp\left\{- \omega'\left[\frac{1}{2}\,\mathrm{sgn}(\omega') - \frac{i}{\pi} \ln|\omega'|\right]\right\} \qquad (2.49)$$

As long as the condition given by (2.44) holds, it is possible to obtain waveshapes for materials with different Q as well as different traveltimes by a combination of scaling and shifting of a single pulse shape. In particular, it follows from (2.46) and (2.48) that the amplitude of the pulse will be approximately proportional to Q. This result, combined with the exact scaling relations (2.37), implies that the function C(Q), defined by (2.38), approaches a constant value as Q becomes large. In order to test the usefulness of (2.38), we have evaluated numerically the value of C(Q). The results are plotted in figure 2.9, for two pulse-width definitions and three different traveltime definitions. These curves show that the value of C(Q) is practically independent of Q, for Q greater than about 20. The similarity of the pulse shape for different values of Q implies that the pulse broadening along the wave path may be summed and (2.38) written as

$$\tau \simeq \int C(Q)\frac{dT}{Q} \simeq C \int \frac{dt}{Q} \qquad (2.50)$$

This relation may provide the basis for a practical method for inverting models for the anelastic properties of rocks *in situ* when the wave sources are sufficiently impulsive and the waves are recorded on broadband instruments. The ambiguities involved in using the pulse breadth in this manner, are far less than those involved in the use of amplitudes in a narrow frequency band, since a number of purely elastic effects, such as focusing from curved interfaces, can have large effects on the amplitudes of seismic signals. This approach also has the advantage over spectral methods that the measurement may be done on a clearly defined phase of the waveform [Gladwin and Stacey, 1974]. It should be noted that equations (2.38) and (2.50) apply for other pulse-width measures than rise time, but the value of C(Q) will of course be different.

Field Measurements of Attenuation

There have been relatively few field studies of the propagation of transient wave pulses in rocks. Gladwin and Stacey [1974] found that the rise time τ, which they defined as the maximum amplitude divided by the maximum slope on the seismogram, could be fitted by an expression of the form

$$\tau = \tau_0 + C\frac{T}{Q} \tag{2.51}$$

where τ_0 indicates the rise time of the source and C was a constant with a value of 0.53 ± 0.04 This value is in reasonably good agreement with the value of 0.485 for large Q predicted on the basis of the CQ theory (figure 2.9).

McDonal et al. [1958] performed experiments in wells drilled into the Pierre shale formation near Limon, Colorado. Fourier analysis of their data indicated that individual Fourier components of the waveforms decayed exponentially in amplitude with distance and that this decay was proportional to frequency. The attenuation per 1000 feet was given in decibels as 0.12 times frequency. Substituting this value into (2.41) and using a velocity of 7000 feet/s gives Q equal to 32. This result was obtained at depths of several hundred feet. Deep reflections indicated that the attenuation decreased with depth with the average attenuation down to a depth of 4000 feet corresponding to a Q of approximately 100. Their waveforms did not show a large amount of broadening over a ratio of 5 in traveltimes; this indicates that the sources were long compared to the impulse response of the wave path so the assumption of a delta function source is not appropriate. However, if the rise times of the waveforms shown in figures 2.3 and 2.6 of McDonal et al. [1958], are

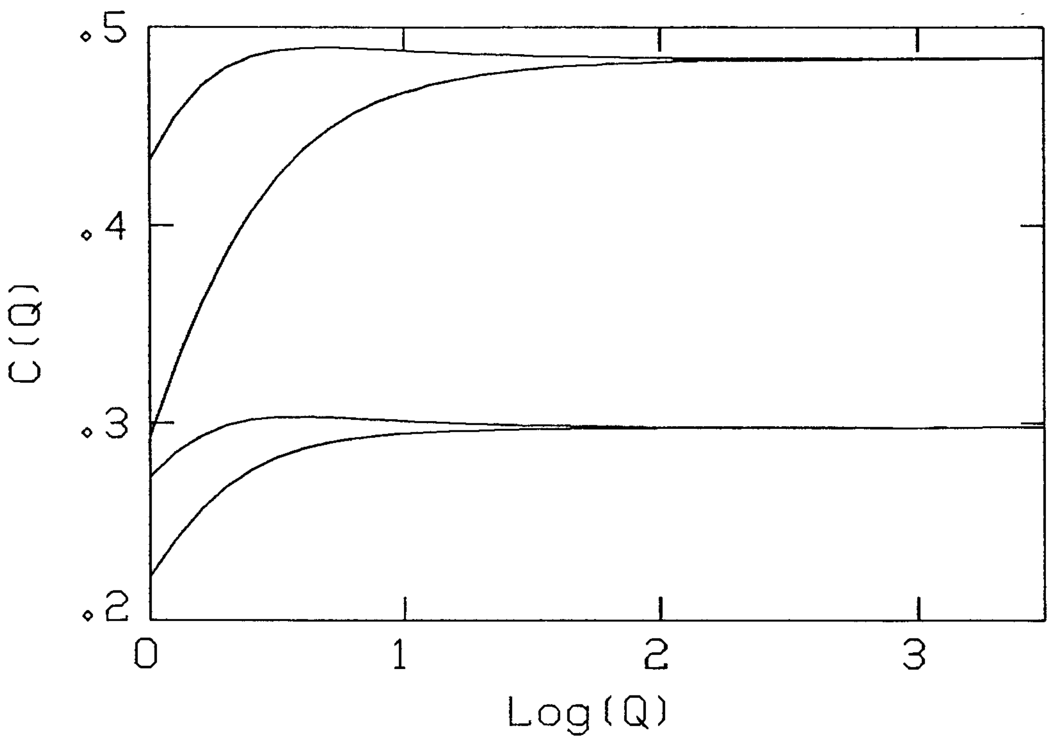

FIG. 2.9. Plot of the function C(Q) defined by equation (2.39). Each pair of curves was computed using a pulse-width measure: the rise-time definition of Gladwin and Stacey [1974], i.e. maximum amplitude divided by maximum slope. The top pair of curves applies to the impulse response b(t), and the lower curve applies to its derivative. The lower curve in each pair was computed using as traveltime T the arrival time of the peak of the pulse, and the upper was computed using the arrival time of maximum slope. The asymptotic values are 0.485 and 0.298.

fitted to the expression (2.51), a reasonable fit may be obtained using C = .5 and Q = 30. This is consistent with the first part of the source being approximately a delta function in velocity or a step function in displacement.

Ricker [1953, 1977] described experiments done in 1948 in the same formation. Waveforms were recorded by three geophones at depths of 422, 622 and 822 feet, for shots at depths less than 300 feet in adjacent wells. Figure 2.10 shows a plot of pulse width vs. traveltime [Ricker 1977; Figure 15.23]. Ricker fitted this data by a function of the form

$$\tau = at^{\frac{1}{2}} \tag{2.52}$$

This relation is in direct conflict with equation (2.37), as well as the experimental result of Gladwin and Stacey [1974]. According to Ricker [1977, p198], this observation is the strongest, if not the only evidence supporting the applicability of his theory to seismic waves. By inspection of figure 2.10 it appears that the data could just as well be fitted by a function of the form (2.51) used by Gladwin and Stacey [1974]. McDonal et al. [1958] criticized Ricker's experiment on the basis that each shot was recorded by no more than three geophones, and that waveforms from different shots were not comparable because, "One cannot shoot a second time in the same hole because the same hole is not there any more." This is probably the reason for some of the scatter in Ricker's data, particularly from the 300-foot shots. This error can be reduced, however, by adjusting the parameter τ_0 in (2.51) for each shot, provided that it is recorded by at least two geophones. Thus we have fitted the wavelet breadth data to a model given by

$$\tau = \tau_{0i} + C \int \frac{dT}{Q} \tag{2.53}$$

In order to facilitate the integration, the traveltime data were fitted to the form

$$T = a(x_g - x_s) + b(x_g^2 - x_s^2) \tag{2.54}$$

where x_g is the depth to the geophone and x_s is the depth to shot. This expression implies that the velocity as a function of depth will be given by

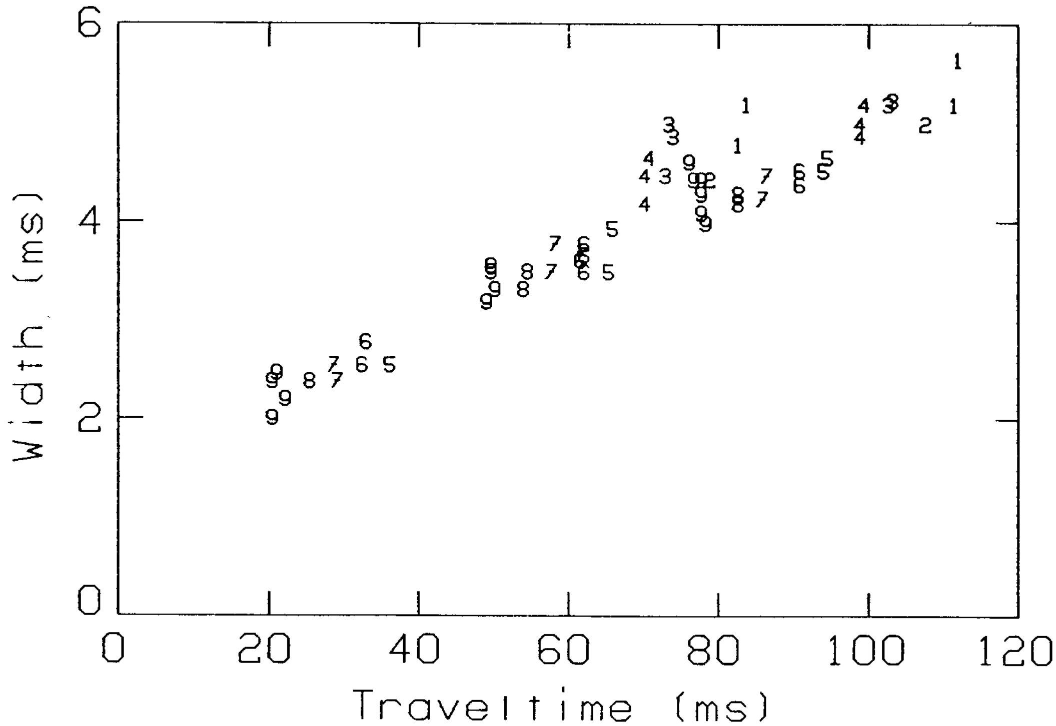

FIG. 2.10. Pulse width as a function of traveltime in Pierre shale. Data from Figure 15.23 in Ricker [1977]. Geophones are at depths of 422, 622, and 822 feet. Sources are at 25-foot intervals at depths from 100 to 300 feet. Numbers indicate sources, 1 for 100 feet, to 9 for 300 feet.

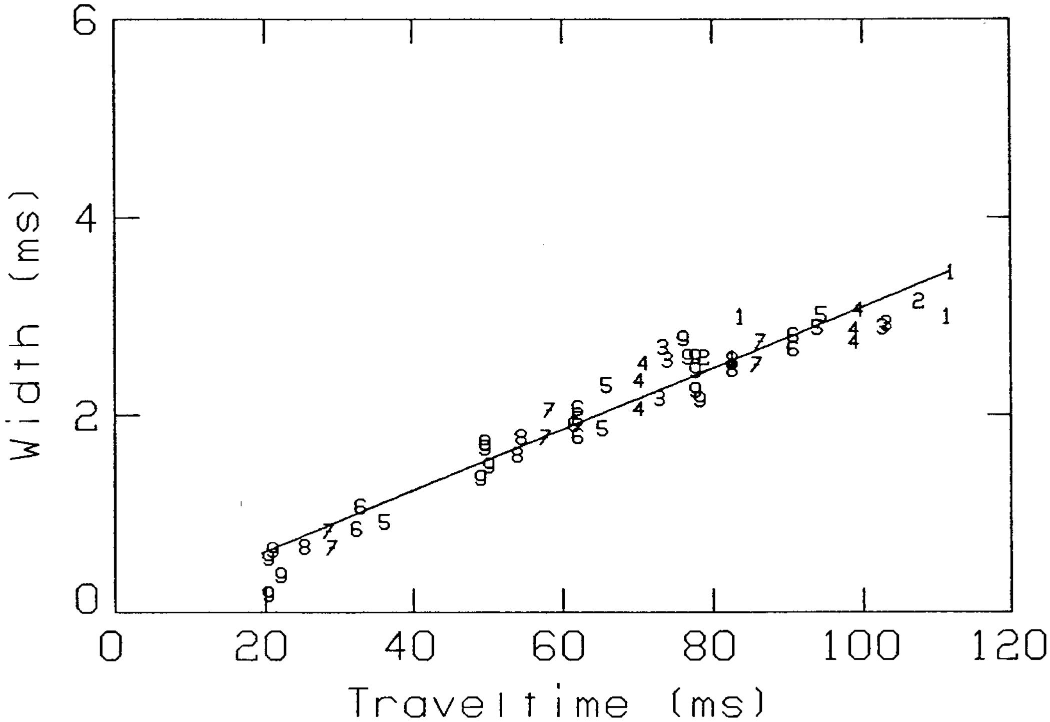

FIG. 2.11. The data in figure 2.10, after subtraction of the initial pulse widths, compared with predicted pulse widths for Q = 32. Both Q and the source widths were determined by simultaneous least-square inversion.

$$V = \frac{1}{a + 2bx} \tag{2.55}$$

As Ricker did not specify which of the data points were obtained from the same shot, it was only possible to determine the source widths for each shot depth. For the pulse-width measure used by Ricker, the value of the parameter C in (2.53) is approximately unity. Figure 2.11 shows a plot of the data from figure 2.10, with the source width subtracted, compared to a straight line with a slope of 1/Q = 1/32. The data points for the geophone at 622 feet tend to be above the curve; this can be explained by attenuation decreasing with depth. This result implies that both Ricker's data and the data of McDonal et al. are consistent with the linear constant Q model, and both give the same value for Q. This is particularly significant in light of the fact that they interpreted their data very differently, and that neither of them considered a constant or near constant linear attenuation in the interpretation of their data. The apparent conflict between the observations of Ricker [1953] and McDonal et al. [1958] has been noted by many authors including Gladwin and Stacey [1974], Reiter and Monfort [1977], and Bless and Ahrens [1977].

Comparison with Nearly Constant Q Theories

Lomnitz [1956] investigated the transient creep in rocks at low stress levels. He found that the shear strain resulting from a step in applied stress could be described to within the experimental error with a creep function of the form

$$\Psi(t) = \frac{1}{M_0}[1 + q \ln(1+at)] \tag{2.56}$$

where a is a frequency much greater than the sample rate or the time resolution of the experiment. He found that the fit to the data was insensitive to the value of a, as long as it was large. For Q greater than about 20, (2.56) is approximately equal to the CQ creep function (2.14). By using the first two terms from the MacLaurin series expansion of the exponential function, (2.14) may be rewritten

$$\Psi(t) = \frac{1}{M_0}\exp[2\gamma \ln(\frac{t}{t_0})] \simeq \frac{1}{M_0}\left[1 + \frac{2}{\pi Q}\ln\left(\frac{t}{t_0}\right)\right]$$

When $t_0 << t$ this is approximately equal to

$$\Psi(t) = \frac{1}{M_0}\left[1 + \frac{2}{\pi Q}\ln\left(1+\frac{t}{t_0}\right)\right] \qquad (2.57)$$

Later, Lomnitz [1957,1962] used his creep law and the superposition principle to derive a model for wave attenuation with Q approximately independent of frequency for large Q. Pandit and Savage [1973] measured Q for several rock samples with Q ranging from 30 to 300 and found good agreement between values determined at sonic frequencies and those derived from transient creep measurements over several tens of seconds.

Kolsky [1956] did experiments on the propagation of ultrasonic pulses in polymers and found the pulse width to be proportional to traveltime. To model his data, he used a viscoelastic model with Q approximately independent of frequency and with a phase velocity that varied according to

$$\frac{c}{c_0} = 1 + \frac{1}{\pi Q}\ln\left(\frac{\omega}{\omega_0}\right) \qquad (2.58)$$

Equation (2.58) follows from (2.43) when the condition given in (2.44) is satisfied. Futterman [1962] arrived at the same formula by imposing causality on the wave pulse and assuming the parameter α in (2.29) to be exactly proportional to frequency over a restricted range of frequencies.

There are two difficulties inherent in Futterman's approach, which necessitate limits on the range where Q is nearly constant, at both low and high frequencies. Collins and Lee [1956] showed that the assumption of a nonzero limit for the phase velocity as frequency approaches zero, implies that Q must approach infinity at zero frequency. Futterman's formulation was based on a finite value of the refractive index at zero frequency and is thus incompatible with constant Q, where the phase velocity has no nonzero limit as frequency approaches zero. It can also be shown [e.g. Azimi et al. 1968], that α proportional to frequency at high frequencies leads to a violation of causality.

It appears that these limitations, which are peculiar to Futterman's approach, have led many workers to assume that a physically realizable formulation with Q exactly independent of frequency was not possible. Liu et al. [1976] and Kanamori and Anderson [1977] have used viscoelastic distributions to derive dispersion relations of the form shown in equation (2.58). Viscoelastic density functions are discussed in appendix A, and it is shown how the constant Q model can be derived from distributions of dashpots and springs.

Discussion

Of the two assumptions that provide the basis for the constant Q model, linearity is the more fundamental, and it has also been more frequently questioned in the literature than the frequency-independence of Q. Nonlinear, rate-independent friction was originally proposed [e.g. Born, 1941] to explain the frequency-independence of Q, since at that time no simple linear models were available that could account for this observation. As summarized in table 2.1, all of the nonlinear friction mechanisms that have been proposed have several features in common. These include the dependence of the effective elastic moduli on strain amplitude, the proportionality of 1/Q to strain at low amplitudes, the frequency-independence of both Q and the moduli, the distortion of waveforms and cusped stress-strain loops, and the absence of any transient creep or relaxation. Mindlin and Deresiewicz [1953] analyzed the losses due to friction between spheres in contact, and found the attenuation to be proportional to amplitude at low amplitudes. White [1966] claimed that the introduction of static friction into this model had the effect of making Q independent of amplitude. This claim cannot be correct since it may be shown [Mavko, 1978] that static friction cannot increase the loss. Walsh [1966] considered the sliding across barely closed elliptical cracks and found the loss for closed cracks with zero normal force to be independent of amplitude. However, this model cannot, as shown by Savage [1969], explain loss independent of amplitude for the whole rock. The required distributions of elliptical cracks would imply that the effective elastic moduli of the rock, as functions of confining pressure, are discontinuous at all values of confining pressure. Mavko [1978] has considered a more general case of non-elliptical cracks and found the attenuation to depend on amplitude in much the same manner as in the contact sphere model of Mindlin and Deresiewicz. All of the above models feature a decrease in the effective moduli with strain amplitude due to the increase in area of the sliding surfaces. Decrease of both velocity and Q, similar to what would be expected on the basis of the above models, has been observed in laboratory studies of rocks, [Gordon and Davis, 1968; Winkler et al., 1979], but only at strains greater than about 10^{-6} to 10^{-5}. At lower strains both Q and wave velocities are found to be independent of amplitudes.

The dependence of the wave velocity on frequency is such that it is difficult to separate it from the effects of spatial heterogeneities. There is, however, an increasing amount of evidence in support of the frequency-dependence of the elastic moduli. Seismic models for the whole earth show much improved agreement with the free oscillation data, when the frequency-dependence of the elastic moduli is taken into account [Anderson et al., 1977]. It is also well established that for many rocks the elastic moduli derived from ultrasonic pulse measurements are significantly greater than the moduli derived from low-frequency deformation experiments [Simmons and Brace, 1965]. This difference is generally larger for lossy materials. Gretner [1961] analyzed well logging data from several oil wells in Canada and found statistically significant differences between observed traveltimes from surface sources to geophones in wells and traveltimes predicted on the basis of high-frequency continuous velocity logs. Strick [1971] showed that these differences could be explained by the dispersion associated with linear attenuation with Q nearly independent of frequency.

Brennan and Stacey [1977] measured both Q and elastic moduli in low-frequency deformation experiments, at strains of 10^{-6}, and found the moduli to vary with frequency as predicted by linearity. The stress-strain loops were elliptical although earlier experiments at larger amplitudes showed cusped stress-strain loops [McKavanagh and Stacey, 1974].

Because the principle of superposition does not apply to the nonlinear solid friction models, it is difficult to predict their effects on the propagation of transient stress pulses. Walsh [1966] pointed out that the losses due to friction cannot be described through the use of complex moduli although this is frequently attempted [e.g. Johnston and Toksoz, 1977]. It is easily shown [e.g. Gladwin and Stacey, 1974] that the use of complex frequency-independent moduli leads to acausal waveforms that arrive before they are excited. Savage and Hasegawa [1967] used the stress-strain hysteresis loops implied by several different friction models, to model wave propagation. The results showed significant amounts of distortion, which have never been observed experimentally.

From these observations it may be concluded that at strain amplitudes of interest in seismology, the propagation and attenuation of waves are dominated by linear effects, with some nonlinear effects showing up at strains of 10^{-5} or greater. This amplitude corresponds to a stress amplitude of 5 bars, since the ambient seismic noise level is on the order of 10^{-11} in strain, and studies of earthquake source mechanisms indicate stress changes of 1 - 100 bars [Hanks, 1977]; it is evident that nonlinear effects can only be significant very near the source.

While a good case can be made for the linearity of the absorption of seismic energy at low amplitudes, no such simple answer can be given to the question of the frequency-dependence of the attenuation. Theoretical models of specific attenuation mechanisms are often formulated in terms of relaxation times, each of which implies a creep function that is a decaying exponential. A model that has a single relaxation time is often referred to as the standard linear solid and has Q proportional and inversely proportional to frequency at high and low frequencies, respectively. Cases where inertial effects may play a role, such as in the flow of low-viscosity fluids [Mavko and Nur, 1979], feature even stronger variation of attenuation with frequency. It may be shown [Kjartansson, 1978] that in materials with sharply defined heterogeneities (e.g. grain boundaries or pores), that absorption due to processes controlled by diffusion, such as phase transformations or thermal relaxation, leads to Q proportional to $\omega^{\frac{1}{2}}$ and $\omega^{-\frac{1}{2}}$ at high and low frequencies, even for uniform distributions of identical pores or crystals.

For these types of mechanisms, the approximate frequency-independence of Q that is observed indicates distributions of time constants, associated with the individual absorbing elements. It may be shown, for example, that the frequency at which maximum absorption occurs for mechanisms involving the diffusion of heat, is inversely proportional to the square of the minimum dimension of the inhomogeneities involved. The empirical observation that Q, in solids, varies much more slowly than even the square root of frequency, is thus an expression of the statistical nature of the inhomogeneities. It is interesting that dielectric losses in solids show the same type of frequency-dependence as do the energy losses in stress waves [Jonscher, 1977].

While Q is probably not strictly independent of frequency, there is no reason to believe that any of the band-limited near-constant Q theories better approximate the wave propagation in real materials than the constant Q model. Therefore, nothing is gained in return for the mathematical complexity and potential inconsistency in using, for example, the absorption band model of Liu et al. [1976].

Strick [1967] obtained a transfer function for wave propagation, of which the constant Q is a special case. He rejected the CQ case, however, on the basis that the lack of an upper bound for the phase velocity was in violation of causality. Strick's three-parameter model is equivalent to the CQ model, with an additional time delay applied to the waveform. Strick [1970] computed waveforms for his models, and found that the detectable onset of the signal always arrived significantly later than the applied time shift. He termed this delay "pedestal" and attributed to it significance that has been subject to some controversy. For the CQ case, the "pedestal" arrives when the source is excited. Minster [1978b] argued that the presence of the "pedestal" was an indication of the need for a high-frequency cutoff of the type built into the model of Liu et al. This "pedestal" controversy points to a limitation shared by all of continuum mechanics; no continuum model, including the CQ model, can have any significance at wavelengths shorter than the molecular separation nor at periods longer than the age of the universe. This covers approximately 32 orders of magnitude in frequency, which for a Q of 100 implies a change in velocity of about 26%. The possibility that some "calculable" energy might arrive 26% earlier than any detectable energy, is hardly a sufficient reason to introduce a high-frequency cutoff. Calculable values of physical parameters, outside the observable range are common in other fields, such as in solutions to the diffusion equation and in statistics. Minster [1978b] and Lundquist [1977] suggest that the cutoff should be at periods between 0.1 and 1 seconds for the mantle. Such cutoffs have never been observed for any of the rocks that have been studied in the laboratory, where the range of frequencies extends up to about one megahertz.

Lomnitz's [1957] attenuation model has often been criticized [Kogan, 1966; Liu et al., 1976; Kanamori and Anderson, 1977] on the basis that the lack of an upper bound for the transient creep would not permit mountains or large-scale gravity anomalies to last through geologic time. Since the Lomnitz creep function is practically equivalent to the constant Q creep function for large values of time and Q, this criticism applies equally to the constant Q model. However, it does not pass the test of substituting numbers into the expressions (2.56) or (2.14). For example, for a material with a Q of 100, the strain that results from the application of a unit stress is only about 33% larger over a period of one billion years, than for the first millisecond of applied stress. Thus, neither the constant Q theory, nor any of the NCQ theories can explain the large strains required by plate tectonics. The fact that brittle deformation only takes place in the uppermost part of the crust, with the exception of localized areas of unusually rapid tectonic activity, may indicate that over geologic time most of the earth deforms as a viscous fluid with Q for shear near zero. The assumption, implicit in the band-limited NCQ model of Liu et al. [1976], that Q approaches infinity outside the range of observations, is thus particularly inappropriate for low-frequency shear deformations in the mantle.

Conclusions

Contrary to what has often been assumed in the past, it is possible to formulate a description of wave propagation and attenuation with Q exactly independent of frequency, that is both linear and causal. The wave propagation properties of materials can be completely specified by only two parameters, for example, Q and phase velocity, at an arbitrary reference frequency. This simplicity makes it practical to derive exact expressions describing, in the frequency-domain, the wave propagation for any positive value of Q. The dispersion that accompanies any linear energy absorption leads to a propagation velocity of any transient disturbance that is not only a function of the material, but also of the past history of the wave. Review of available data indicates that the assumption of linearity is well justified for seismic waves, but it is likely that Q is weakly dependent on frequency. There is, however, no indication that any of the NCQ theories that we have discussed provide a better description of the attenuation in actual rocks than the constant Q theory does.